CHEMICAL ENGINEERING TRANSACTIONS
VOL. 46, 2015

A publication of AIDIC
The Italian Association of Chemical Engineering
Online at www.aidic.it/cet

Guest Editors: Peiyu Ren, Yancang Li, Huiping Song

ISBN 978-88-95608-37-2; **ISSN** 2283-9216
DOI: 10.3303/CET1546075

Forward Modelling and Detection of GPR in Urban Road Base Disease

Yanwei Bao*[a], Ruixia Gao[a], Dong Guo[a], Shanshan Bai[a], Xiangjing Xin[b]

[a] Handan Polytechnic College. Handan Hebei, China
[b] Kailuan Group Limited liability company Tangshan Hebei, China
ffbyw@163.com

Ground penetrating radar is a high-resolution engineering geophysical method which has better detection effect to disengaging, cavities and leakiness in urban road base. This paper is based on the principle of ray tracing through the forward modelling of urban road base hollow, empty and not dense disease, analyses waveform, frequency, wave propagation characteristics of primary disease forward image simulation. The paper summarizes the urban road base diseases in ground penetrating radar profile feature of signal, and analyses field exploration radar profile and further research on primary diseases of urban road ground penetrating radar fingerprint for urban road base disease detection of ground penetrating radar data interpretation to provide the reference.

1. Introduction

Urban road has developed quickly with the rapid development of the national economy. Urban road network can be gradually improved and the quality of the road can be improved continuously. The development of the urban road can promote the rapid growth of urban economy and bring huge social benefits to the city. However, the disengaging, cavities and leakiness and other diseases are caused by the road construction, vehicle load, underground pipeline breakage and underground engineering construction .etc. Due to the existence of hidden in the road structure, these diseases existing in the road base and the subgrade are difficult to detect and deal with in time and these diseases have not been discovered until the road has collapsed and subsidence, which has affected the safe operation of the road.
GPR is a high resolution engineering geophysical method which can detect the urban diseases quickly and effectively [1][2][3]. The detective technology of GPR uses time cross-section formed by the strati-graphic medium reflection wave superposition to analyse and image analysis results depend on a large number of field tests and technical personnel's experience. So there are many uncertain factors which may affect the results of the detection. In this paper, the forward modelling of the common diseases of urban road GPR images is carried out and the characteristics of the forward image of different diseases are analysed to improve the accuracy of the data interpretation.

2. Basic principles of GPR detection

GPR road diseases principle, as shown in Figure1. A series of Electromagnetic Impulse emitted from the transmitting antenna, Electromagnetic Impulse generates reflection on 3 interfaces R_0 , and R_2 , a portion of energy of is reflected on the interface of R_2 , the other part is transmitted down to the next interface gradually. If the interface is uniform, the incident will continue to be transmitted downward and the reflection phenomenon will not appear. When there is an abnormal body in the roadbed, the electromagnetic wave reach the edge point A of the disease anomalous body firstly. Because the dielectric constant of the roadbed is greater than the cavity dielectric constant (there is only air cavity), only part of the wave energy is reflected by the interface to the base course and the surface course, and reaches to the air layer. In this moment, the trip distance of the electromagnetic waves is longer than the distance between the surface layer and the grass root, so the travel time is longer, and the waveform changes can be seen in the instrument. After reaching to the Point A, the electromagnetic waves continued to move forward to the interface of Point B which formed the normal reflecting surface of $\varepsilon_0 < \varepsilon_3$, which the waves can be reflected in the roadbed disease, and lastly also into the

Please cite this article as: Bao Y.W., Gao R.X., Guo D., Bai S.S., Xin X.J., 2015, Forward modelling and detection of gpr in urban road base disease, Chemical Engineering Transactions, 46, 445-450 DOI:10.3303/CET1546075

air layer when the reflection reach to the base layer and surface layer, and the travel time is t_B . Then there was a time of mutation, the changes of the waves also can see in the instrument. The travel time $t_B > t_A$, the increment $\Delta_1 = t_B - t_A$, likewise, $\Delta_2 = t_M - t_N$, can also have Δ_3 , ... Δ_n . This not only can see the changes of the waveform in the instrument, but also can get the information such as the disease types, location, range and severity.

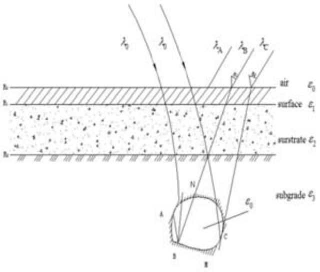

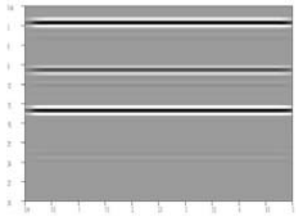

Figure 1: The principle chart of road diseases of GPR *Figure 2: Intact road constructions on simulation*

3. Forward modelling of GPR in urban road base disease

The GPR can detect the road diseases, such as the disengaging, cavities and leakiness in urban road base and so on, which have different signals and image features on the radar cross-sectional drawn, mainly reflect in the waveform phases, amplitude, frequencies and other features [4][5][6].

The ray-tracing method plays a very important role in the model test, back calculation and tomography technique, which has the characteristics of the quick speed in calculation and visual results and has been widely used in wave propagation problems [7][8][9] [10][11][12] This paper used the ray-tracing method for the common urban road base diseases to forward modelling, analysed the results, and included the features and regularity of the radar signal on different urban road base course.

3.1 Intact road construction simulation

Intact road construction is that every medium in the facial layer, base layer, mat layer and roadbed is equally distributed, less changed and not significantly difference, and the snow attenuation of the electronic wave which only have more significant reflection in the interface of the structure layer, as shown in Figure 2.

3.2 Disengaging disease simulation

3.2.1 Air disengaging

Design of forward modelling on the air disengaging disease is shown as Figure 3, whose length is 10m and depth is 0.77m. There are 6 air inflatable disengaging model with the same length and different height in the position where is the interface near the top of base layer, and the range of disengaging shown in Table 1.

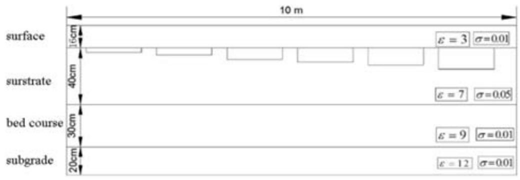

Figure 3: Diagrammatic drawing of air disengaging disease

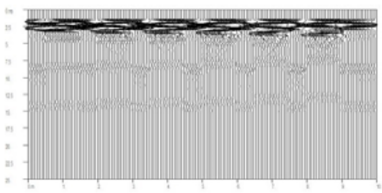

Figure 4: Forward modelling of air disengaging diseases

Table 1: The parameter table of the range of disengaging disease

Number	T1	T2	T3	T4	T5	T6
L(m) × W (m)	1×0.03	1×0.05	1×0.08	1×0.10	1×0.12	1×0.15

How to use the GPR to distinguish the volume of disengaging is also one of the key content of the research. According to the theory of electromagnetic fields of GPR, when the disease reaches the 1/4 of disengaging wavelength, it can be identified and calculated the volume from the phase change, and the velocity of the electromagnetic wave is 0.3 m/ns. The wavelength application parameters are shown in the table 2 if the antenna is the 900MHz.

Table 2: Parameter table of 900MHz antenna wavelength changes with depth

Attribute	Full wavelength	1/2 wavelength	1/3 wavelength	1/4 wavelength	1/5 wavelength	1/6 wavelength	1/7 wavelength	1/8 wavelength
Size(m)	0.333	0.167	0.111	0.083	0.067	0.0556	0.0486	0.042

From the table2, when the disengaging range reaches 0.08m, theoretically, the radar cross-sectional view can be distinguished. At the same time from the phase analysis, when there is disengaging disease in the road, its top reflector and the incident electromagnetic wave phase is same, but the bottom phase is opposite.

From the radar cross-sectional view on the forward modelling, we can more clearly distinguish the reflection of top and bottom interface in 15cm disengaging zone which is approximate1/2 wavelength. For the 10cm disengaging approximate 1/3 wavelength, the bottom interface is not clear due to superposition of the reflection wave of the bottom interface of disengaging region and the reflection of the top interface delay, but it can be judged by the inflection point of the time position reflected by the bottom surface. The disengaging of 12cm in the radar forward modelling cross-sectional view can be distinguished the top and bottom interface.

The disengaging, approximate 1/4 wavelength, is 8cm, compared to the disengaging of 10cm, whose inflected signal in the bottom interface is more difficult to distinguished and the change of the inflection point was obviously weakened. When the disengaging is 5cm and 3cm, namely the disengaging reduce to 1/6 wavelength, this time the reflection signal is superimposed to form a complete sub-wave morphology, it is difficult to distinguish between top and low interfacial reflection in the forward modelling of radar

3.2.2 The water-filling disengaging

The model of water-filling disengaging disease is shown in Figure 5. Its length is 4cm and its depth is 0.77m. Three different water-filling models were set up in the base layer near to the interface of the facial layer.

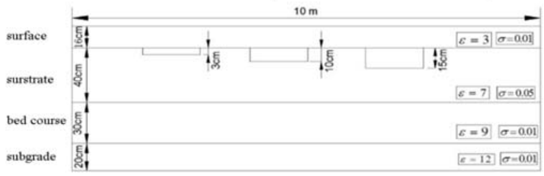

Figure 5: The diagrammatic sketch of water-filling disengaging disease model

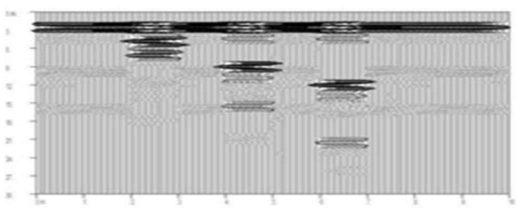

Figure 6: The mimic diagram of water-filling disengaging disease forward modelling

As shown the results of water-filling disengaging disease forward modelling that the phase of the top reflection in the water-filling disease area is opposite to the radiated electromagnetic waves. Because the permittivity of water is large, speed is low, its wavelength is about 1/10 in the air, approximately 0.3m/ns , the 3cm water-filling area can be distinguished from the resolving power of 1/4 wavelength. Because the water-filling cross sectional view has a strong presence of multiple waves, there is a strong interference with signal of the disengaging area below.

3.3 Modelling of the cavity disease

Roadbed cavity disease is one of the main causes of pavement collapse, so the detection of disengaging disease also is the key research content of road detection. The distribution range is larger than the disengaging disease, and mostly distributes in the roadbed. As shown in Figure 7, the length of model is 7m and depth is 1.57m. There are 5 different sizes cavities in the roadbed layer and the medium filled is air. Forward modelling is shown as Figure 8 and Figure 9, which used separately 900MHz and 400MHz antennas. As shown in the results of forward modelling, 400MHz and 900MHz antennas can be reflected unusually on the radar cross-sectional view of the modelling GPR, and the cavity is bigger, the reflection is more obvious; the frequency of antenna is higher, the abnormal of the radar cross-sectional cavity is more obvious. The multiple waves of subgrade cavity is strong for some time, the cross-range scattered wave is not strong and have part and isolated features, the phase of reflection is the same tendency as the incident wave, but it is opposite to the reflected wave on the surface of the roadbed.

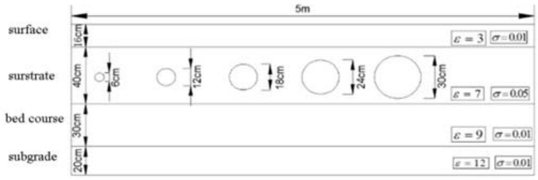

Figure 7: The diagrammatic sketch of cavity disease model

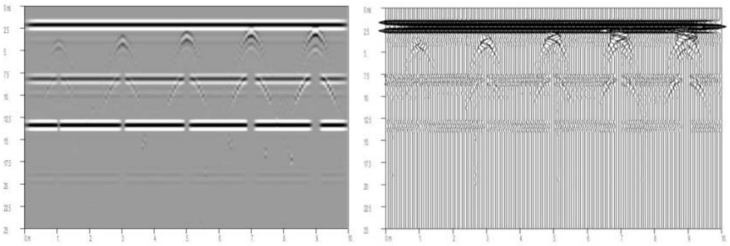

Figure 8: The mimic diagram of 900MHz antenna cavity disease forward modelling

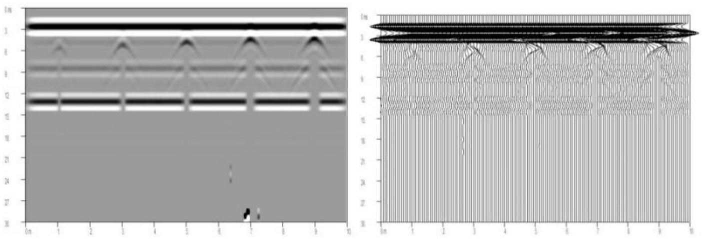

Figure 9: Forward modelling mimic diagram of cavity disease

3.4 The modelling of roadbed leakiness

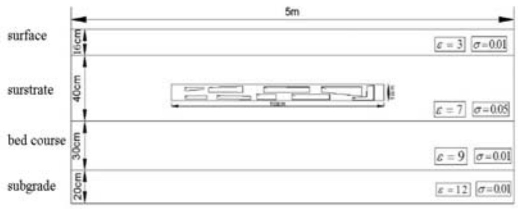

Figure 10: The model of roadbed leakiness

If compaction of the road is unqualified, it will cause the aggregate loose and make the roadbed leakiness. Because the high porosity or moisture content in the leakiness area will cause the road collapse, subsidence, disengaging and cavity, etc. under the repeat loading. The leakiness model of roadbed is shown as Figure 10. The results of the forward modelling (Figure 11) show that the electromagnetic waves under the leakiness disease area will produce strong reflection and definite diffraction, the disorder waveform, the poor regularity and the poor coherence compared to the event. There are negative wave crest and positive wave crest in forward simulation map because of the presence of disease pore region, So the electromagnetic wave propagation process will undergo two changes of dielectric constant from small to large and and from big too small.

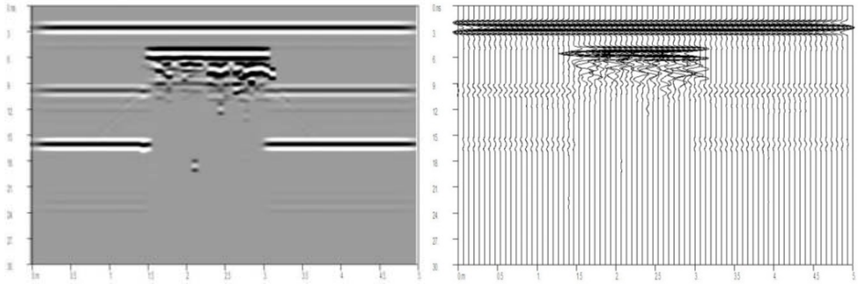

Figure 11: Forward modelling of roadbed leakiness disease

4. Ground penetrating radar image analysis

The image of measured radar cross-sectional view influenced by the factor of environment and the geologic status is different from that of forward modelling, but the results of forward modelling summarized the different diseases' electromagnetic features which have a guide meaning to the interpretation of the measured radar data.

A road is bituminous pavement. The bituminous pavement was overplayed the original cement concrete pavement. The layered interface of pavement, base and subgrade can be distinguished clearly in the figure, where the roadbed is more completely dense, there is no strong reflection in the profile, continuous phase axis; Due to the different dielectric constants of base and subgrade materials, the interface of base and subgrade has strong reflection, Strong reflection of the arc that the incident reverse phase and waveform phase and there are multiple waves, occurs in the ground 1m, so there was speculated as water filling concrete pavement diseases.

From the radar detection section of the other part of the road, the asphalt road surface in the figure, the original cement concrete pavement layers, base and subgrade layers. The base is relatively complete, compact, continuous phase axis and it does not appear strong reflection; There is a strong reflection because the material permittivity difference between the base and the sugared is bigger; Phenomena that the waveform is disordered, poor regularity, poor correlation with axes, strong reflection, diffraction alternately appear at the bottom-left , showing no compacting subgrade; When there is multiple strong arc-shape reflections at the lower right, we may determine that is the abnormal pipeline according to the data.

5. Conclusions

(1) The antenna of 900MHz can identify the disengaging volume above 0.08m and can identify the emission of top and bottom interface of the disengaging area. Its top reflector is the same as the incident electromagnetic wave phase, while the phase of the bottom is opposite when disengaging diseases existed in the road.

(2) The GPR can identify the 3cm of water-filled disengaging areas, whose top reflector is opposite to the phase of the radiated electromagnetic wave. There is a strong presence on the water-filled disengaging sectional view which made a stronger interference to the following signal in the disengaging area.

(3) The disengaging diseases on the sectional view is arc-shaped, or like arc. The more obvious the cavity is, the higher the antenna frequency is, the more obvious And the more obvious is the disengaging abnormity in the radar sectional-view. Therefore, the phase of reflection is the same as the incidence and is opposite the reflection wave of the roadbed layer.

(4) When the base layer occurs leakiness, the radar sectional-view appears phenomenon such as the poor coherence of the axes discontinuity, the disorder waveform, diffraction and lacking regularity etc.

(5) GPR could be greatly influenced by the surrounding environment when it is detecting the urban road. For example, Such as different type underground pipelines, the transmission lines and mobile signal towers, which will interfere with the processing and interpretation of ground penetrating radar detection data? These interference factors must be recorded in the field of detection so that these could be reduced and eliminated in processing and analysing data to increase the reliability.

References

Cao X.S., Cai L., Zheng C.J., 2002, Application of GPR in highway quality inspection and management [J]. Journal of Hohai University (Natural Sciences, 30(3): 68-71, DOI: 10.3321/j.issn: 1000-1980.2002.03.016.

Carcione J.M., 1998, Radiation patterns for 2-D GPR forward modelling [J]. Radio Science, 63(2): 424, DOI: 10.1190/1.1444342.

Cui A.L., Liu K.H., 2008, Application of ground penetrating radar (GPR) technology in karst survey [J]. Journal Of Earch Sciences And Environment. 30(2) 197-199, DOI: 10.3969/j.issn.1672-6561.2008.02.016.

Feng D.S., Dai Q.W., He J.S., He G., 2006, Finite difference time domain method of GPR forward simulation. Progress in Geophysics. 21 (2): 630-636, DOI: 10.3969/j.issn.1004-2903.2006.02.046.

Liu J., 2006, Application of geophysical radar technology to inspecting existing railway [J]. Railway Engineering (10): 77-78, DOI: 10.3969/j.issn.1003-1995.2006.10.030

Qin H., Qiu H., Yang T.W., 2012, Analysis of GPR image in advanced Geological forecast for tunnels [J]. Site Investigation Science and Technology (2): 57-61, DOI: 10.3969/j.issn.1001-3946.2012.02.015.

Wang C.B., Ding W.Q., You G.M., 2007, Technology and application of advanced geological prediction in tunnel [J]. Hydrogeology and Engineering Geology. (1): 120-122, DOI: 10.3969/j.issn.1000-3665.2007.01.027.

Wu X.N., 2011, Application Of Ground Penetrating Radar in Detection for Cavity Defects of Pavement [J]. Technology Of Highway And Transport. (1) 33-36, DOI: 10.3969/j.issn.1009-6477.2011.01.009.

Xiao H.Y., Lei W., Yang W., 2008, Correspondence between geological characteristics or radar images and typical geological phenomenon [J]. Coal Geology & Exploration. 36 (4) 57-61, DOI: 10.3969/j.issn.1001-1986.2008.04.015

Xu S.C., Liu F., 2000, The research and application of GPR to detect thickness in city road [J]. Journal Of East China Jiaotong University. 17(4) 24-28, DOI: 10.3969/j.issn.1005-0523.2000.04.007.

Yang T.C., Li S.L., Wu Y.G., 2001, Theory and application of prospecting pavement structure by ground-penetrating radar [J]. Journal of Central South University of Technology (Natural Science) 32 (2): 118-121, DOI: 10.3969/j.issn.1672-7207.2001.02.003.

Zhao J.S., Guo Y.K., Tang P.Y., Peng T.J., Qian S., 2003, The experimental researches of comprehensive damage-free sugared quality inspecting technology [J]. Journal Of Changsha Railway University, 21(3): 34-38, DOI: 10.3969/j.issn.1672-7029.2003.01.007.